Exploring Potentialities and Limitations of Stapled *o*-Oligo(PhenyleneEthynylene)s (*o*-OPEs) as Efficient Circularly Polarized Luminescence Emitters

Pablo Reiné,[a]José Justicia,[a]Sara P. Morcillo,[a]Giuseppe Mazzeo,[b]Emilio García-Fernández,[c]Antonio Rodríguez-Diéguez,[d]Luis Álvarez de Cienfuegos,[a]Sergio Abbate,[b] Juan M. Cuerva,[a]Giovanna Longhi*[b] and Delia Miguel*[c]

Abstract: In this paper we have studied the chiroptical properties of a family of *o*-OPE derivatives with different steric hindrance. Experimental results show high dissymmetry factors (g_{abs} and g_{lum} up to $1.1x10^{-2}$) and very similar ECD and CPL for all the derivatives, that makes this basic *o*-OPE scaffold a robust pure organic emitter. VCD spectra are used to characterize conformational properties in solution. DFT and TD-DFT calculations support experimental results also proving that ECD and CPL are almost exclusively linked to helical moiety and not to size or conformation of substituents. As chiroptical properties of these emitters are independent of substituents, this OPE scaffold can be used as basic skeleton for the design of sensing probes with high CPL efficiencies.

Keywords: enantiopure organic emitters, chiroptical properties, ECD, CPL, VCD

Introduction

Light emitting compounds have attracted the attention of scientists along the years owing to their very different and useful applications. Within this context, it is known that chiral fluorescent compounds are able to emit light with some degree of circular polarization. This property is commonly described as circularly polarized luminescence (CPL)[1-6] and has been proposed as the basis for the development of advanced optical luminescent devices.[7-13] The degree of circular polarization of emitted radiation is usually characterized by the luminescent dissymmetry factor $g_{lum} = 2(I_L-I_R)/(I_L+I_R)$, being the I_L and I_R the intensities of the left and right circularly polarized light.

[a] *Department of Organic Chemistry*
University of Granada
C.U.Fuentenueva, Avda. Severo Ochoa s/n Granada

[b] *Corresponding Author giovanna.longhi@unibs.it*
Dipartimento di Medicina Molecolare e Traslazionale,
Universitá di Brescia
Viale Europa 11

[c] *Corresponding Author dmalvarez@ugr.es*
Department of Physical Chemistry
University of Granada
C. U. Cartuja, C/ ProfesorClavera s/n Granada

[d] *Department of InorganicChemistry*
University of Granada
C. U. Fuentenueva, Avda. Severo Ochoa s/n Granada

Received: ((will be filled in by the editorial staff))
Revised: ((will be filled in by the editorial staff))
Published online: ((will be filled in by the editorial staff))

Therefore, the search for new and efficient CPL-emitting compounds is now a growing research field. Among all the potential emitting structures, the development of single organic monomolecular (SOM)-emitters[14-28], with reasonable dissymmetry factors, is very appealing. Thus for example, they have been suggested as crucial materials for the development of CP laser emmision.[29] Recently, we described a new class of such SOM-emitters[30] based on stapled *o*-oligophenylenethynylene (*o*-OPE)-derivatives.[31] These very simple structures show a considerably luminescent dissymmetry factor (g_{lum}) reaching 0.01 at the maximum of the emission. This value is very unusual for SOM-emitters, especially if we take into account the apparent flexibility of their backbones. We wondered if this value could be increased/modified making the structure more rigid or including new dissymmetry in the structure. Quite interestingly, the two hydroxyl groups located in the staple allow an extra functionalization / derivatization of these o-OPEs opening the door to elaborate CPL emitters with new properties. To this end, we selected as starting material enantiopure diol (*P,S,S*)-**1**, which gave the best g_{lum} value in our previous work.[30] We then prepared derivatives **2-6**, with increasing volume (**1**, R = H; **2, 3**, R = Ac; **4, 5**, R = Piv; to **6** R = OTBDMS) in the pendant groups in order to make structure more rigid. Moreover, the monofunctionalizated products **2**, **4** and **6** resulted in asymmetric products instead of the original symmetric one.

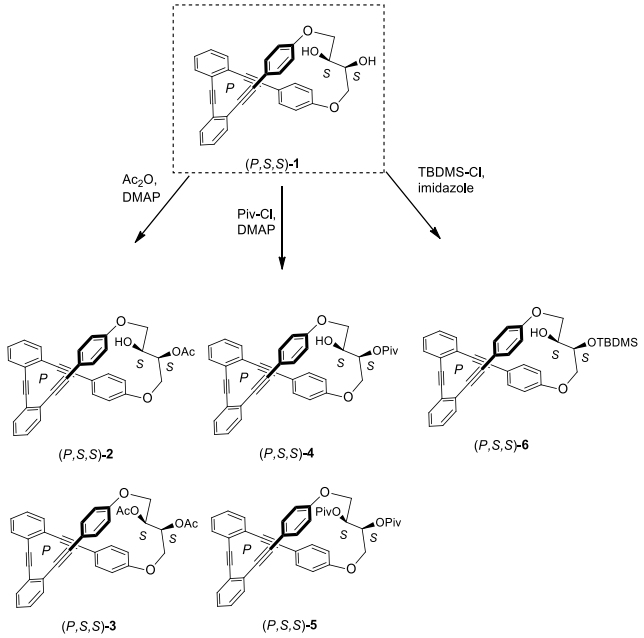

FIGURE 1 Structures of (*P,S,S*)-**1**-**6**.

In this work we aim to report on the effect of such structural modification in the dissymmetry factor of the CPL trying to push these systems to the limit and to extract some hints about the origin of their excellent CPL behavior. In this way, guidelines for the development of a new generation of emitters with better CPL properties could be obtained.

Results and Discussion

Synthesis and characterization of compounds (*P,S,S*)-2-6

Compounds (*P,S,S*)-**2**-**6** were prepared from enantiopure diol (*P,S,S*)-**1** by simple esterification and silylation reactions. In the case of *tert*-butyldimethylsilyl derivative (*P,S,S*)-**6**, the bulkiness of the *tert*-butyldimethyl silyl subunit prevents the preparation of the bis-silyl derivative. Suitable crystals for X-ray monocrystal diffraction were obtained by slow diffusion of hexane to a CH_2Cl_2 saturated solution of (*P,S,S*)-**5**. In this way, the structure of (*P,S,S*)-**5** could be fully resolved showing the helical arrangement and, remarkably, the stereochemical relationship between the *P* chiral helicity and the (*S,S*) diol chirality. It is worth noting that for diol (*P,S,S*)-**1** the stereochemical assignment was previously established, based on theoretical calculations.[30] This result validates all our theoretical approximations and findings.

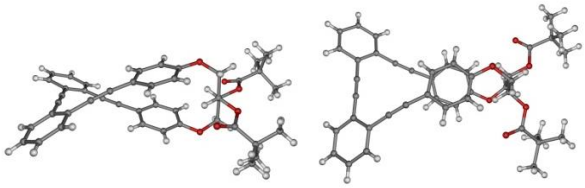

FIGURE 2. Side (left) and top (right) views of X-ray structure of compound*(P,S,S)*-**5**.

Optical properties of compounds (*P,S,S*)-2-6

Absorption spectra of these compounds present two maxima at c.a. 280 and 300 nm and a shoulder at 340 nm. As it can be seen in Figure 3a, the introduction of one and two bulky substituents in the hydroxyl groups gives no appreciable differences in shape and intensity of absorption spectra. A similar behaviour is observed in fluorescence spectra, where a maximum at around 410 nm is observed for all the derivatives (Figure 3b). They are also fluorescent in different (apolar, polar, protic and aprotic) solvents with quantum yields (Φ) ranging from 0.12 to 0.52 (See Supporting Information). In all cases, the time resolved emission spectroscopy (TRES) analysis resulted in two lifetimes around 4 and 1 ns. This result is similar to that previously reported by us for compound (*P,S,S*)-**1** (See SI for details).[30]
Good quantum yields combined with large absorbances are needed for practical applications. For most of the compounds the highest quantum yield was obtained in CH_2Cl_2 solutions, so we selected this solvent to carry out the study of chiroptical properties.

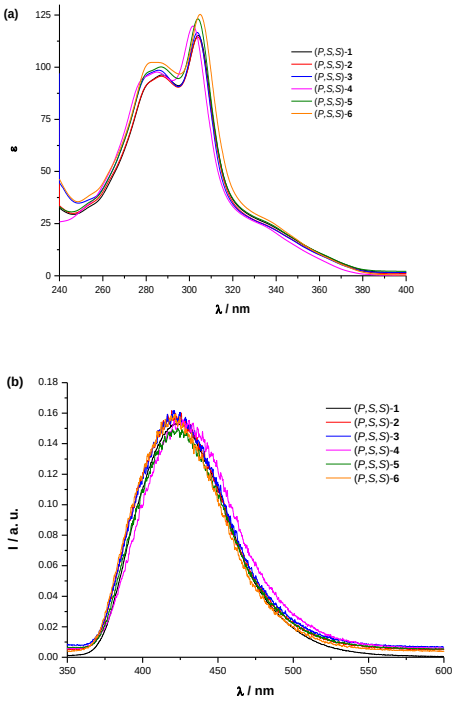

FIGURE 3. (a) Absorbance and (b) emission spectra of compounds *(P,S,S)*-**1-6**.

Chiroptical properties of compounds (*P,S,S*)-2-6

ECD

All the new compounds, (*P,S,S*)-**2**-**6,** exhibit a remarkable chiroptical response with intense Cotton effects at 280, 300 nm and between 340-390 nm in the same way as the parent (*P,S,S*)-**1**. Sign and intensity of circular dicroism (Δε) at the longest wavelengths are very similar in all the cases, with a value around +100 (Figure 4a). Remarkably the associated g_{abs} values, defined as $g_{abs} = (\varepsilon_L-\varepsilon_R)/\varepsilon$, for that S_0-S_1 transition also ranges from 0.9 x 10^{-2} for diol (*P,S,S*)-**1** to 1.2x10^{-2}, for monopivaloyl derivative (*P,S,S*)-**4** (Figure 4b). These values suggest that if the structure is retained in the excited state good g_{lum} values may be obtained in the S_1-S_0 emission.

Taking into account the previous X-ray structure of (*P,S,S*)-**5** (Figure 2) and its positive sign of the Cotton effect at λ = 345 nm we can confirm our previous assumption that, in these structures, the absolute configuration of the helix can be extracted from the ECD in the same way as in [n]-helicenes.[32]

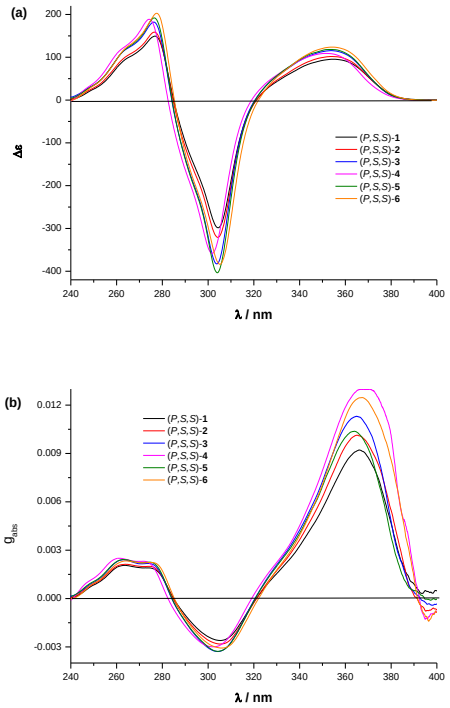

FIGURE 4.(a) ECD and (b) g_{abs} spectra of compounds *(P,S,S)*-**1**-**6**.

To extract more information about these structures we theoretically studied compounds *(P,S,S)*-**2**-**6**.

Accurate molecular mechanics (MM) conformational search was performed for all OPE molecules, assuming (1*S*, 2*S*) configuration for all the compounds. Calculations were performed at B3LYP/6-31g* level, treating solvent effect with iefpcm method.

DFT calculations suggest that in all cases for the (*1S, 2S*) enantiomer the *P* configuration is favoured, as reported in SI (Tables S4-S8). Conformational search in monoacetylated (*P,S,S*)-**2** showed four different energetically accessible conformers, one of them (conformer 4, 88.3% population, Figure 5a) being clearly favoured. The calculated UV-vis and CD spectra for such conformer also fit well with the experimental ones in Figure 4.

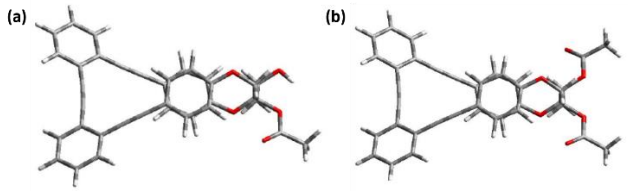

FIGURE 5. Main conformer of optimized geometry of (a) (*P,S,S*)-**2** and (b) (*P,S,S*)-**3**.

From a structural point of view, it shows an almost perfect helical geometry, which seems to be the reason of the observed high g_{abs} values (See SI for details).

Symmetric compound (*P,S,S*)**-3** presented a simpler conformational space dominated by only one conformer (99.3% of conformer 1, Figure 5b). As expected, the simulation for the corresponding UV-vis and CD spectra gave again an excellent match with the experimental one. The similarities between those spectra and the ones obtained for (*P,S,S*)-**2** can be understood in terms of very similar geometries. In fact, structures of main conformers are almost superimposable.

For the other derivatives (*P,S,S*)-**4**-**6** similar results were obtained. From all of these TD-DFT calculations it is clear that the CD spectrum is exclusively derived from the OPE helical backbone, and that is influenced neither by the conformation of the aliphatic bridge, also in presence of substituents with steric hindrance, nor by the local conformations of the substituents. On the other hand, the helicity of the OPE backbone is only driven by the configuration of the two asymmetric carbons of the bridge. Theoretical findings also confirm the identical behaviour of the ground state for all the studied compounds as experiments suggested. All simulations are summarized in Figure 6.

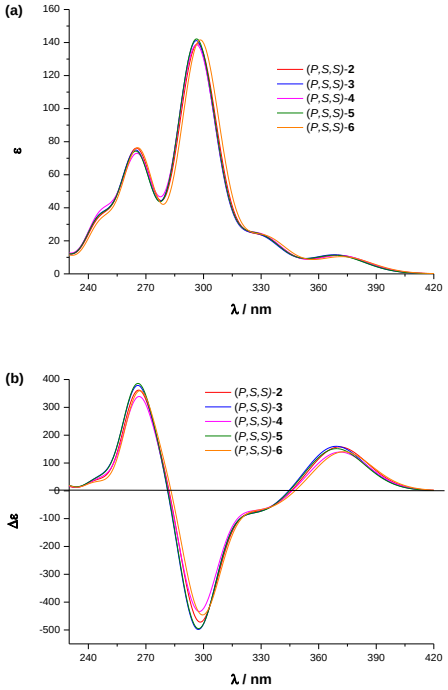

FIGURE 6. TD-DFT calculated (a) UV-vis and (b) ECD spectra of *(P,S,S)*-**2**-**6** (iefpcm B3LYP/6-31G*, Gaussian bands with half bandwidth 0.16 eV). For sake of comparison with experiment calculated spectra have been redshifted by 30 nm.

CPL

As it can be seen in Figure 7, the CPL response of compounds (*P,S,S*)-**2**-**6** remains practically identical to that obtained for diol (*P,S,S*)-**1**, despite the functionalization degree and different symmetries. Consequently, they present g_{lum} values with a maximum of 1.2 x 10^{-2} at 390 nm. It is known that luminescent dissymmetry factor is not in general a fixed parameter for the entire emission band.[1] In this case, g_{lum} presents a maximum value which is slightly shifted with respect to the maximum of the emission. At the maximum of the emission (400 nm) a g_{lum} value of 1x10^{-2} is observed. These results show that diol (*P,S,S*)-**1** is an excellent scaffold for the construction of more complex luminescent structures.

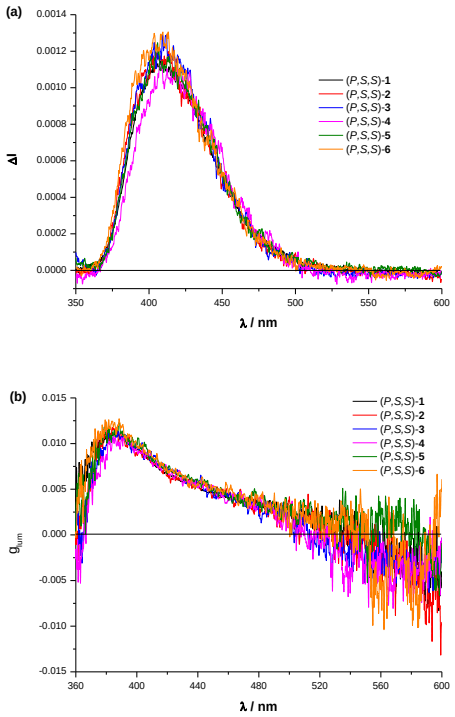

FIGURE 7. (a) CPL and (b) g_{lum} spectra of *(P,S,S)*-**2**-**6.** Data for diol *(P,S,S)*-**1** has been included for comparison.

We also checked the behaviour of selected compound (*P,S,S*)-**5** in different solvents, and obtained almost identical responses, which suggests that these systems present a conformational equilibrium in which one of the conformers is much more stable than the others independently of the nature of the solvent. Consequently, the CPL spectra are also very similar in all the tested solvents (See SI for details).

To understand the origin of the high g_{lum} values in these structures new calculations were carried out using in this case the parent compound (*P,S,S*)-**1**. Evidences from TRES measurements suggest that emission is faster than the interconversion among different conformers. Analogous dynamic situation was in fact explored previously by us as the basis of a chiroptical switch.[30] For this reason it is worthwhile to study by TD-DFT calculations the excited state structure.

The optimized geometry of the first excited state of the most populated conformer was then calculated and compared with the optimized geometry of the ground state of the most populated conformer. Rotational strengths for the S_1-S_0 transition were also calculated. As far as the structure is concerned, both ground and first excited states are quite similar (Figure 8), as experimental data suggest. In parallel with the longer wavelength associated to the transition in emission, a change in conjugation is observed as well as lengthening of triple bonds and CC bonds of the aromatic rings. The distance between the two carbon atoms 1 and 2 on the opposite phenyl rings gets shorter in the excited state, the dihedral angle 1-2-3-4 (see Figure 8 for definition) increases slightly (see SI). These observations are general and tested using different basis sets and the two functionals B3LYP and CAM-B3LYP (See SI).

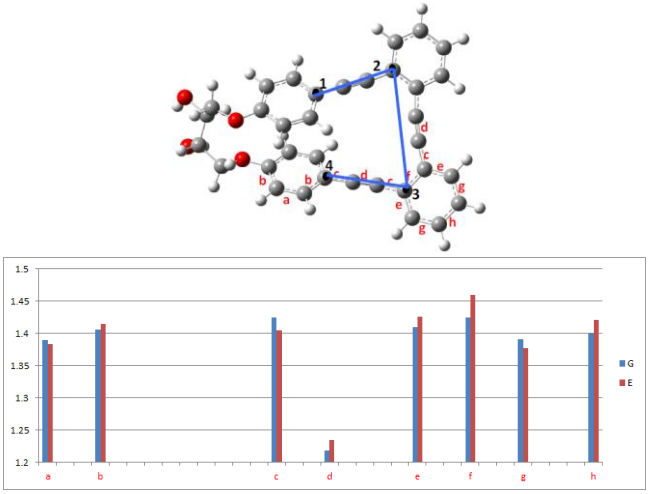

FIGURE 8. 3D Structure of the first excited state of (*P*,*S*,*S*)-**1** and comparison of CC bond lengths of the OPE moiety in the ground (G) and excited state (E) geometries (B3LYP/6-31G* level); more extended basis set confirm these data. There is some dependence on the functional when comparing B3LYP with long range corrected functionals, like CAM-B3LYP (see SI for a discussion)

The shape of the orbitals responsible of the CPL is also very informative. They are mainly located far from the staple, which is in accordance with the insensitivity of the emission with respect to the nature of the staple (Figure 9). On the other hand, the dissymmetry of the emission relies in the torsion angle and probably length of a particular moiety in the structure, which show some hints about how to improve the CPL emission in these compounds maintaining a functionalizable part on them. Moreover, comparison of the HOMO-LUMO orbitals involved in the first absorption transition and in the emissive transition shows a strong similarity in agreement with the experimentally observed similarity between g_{abs} and g_{lum}.

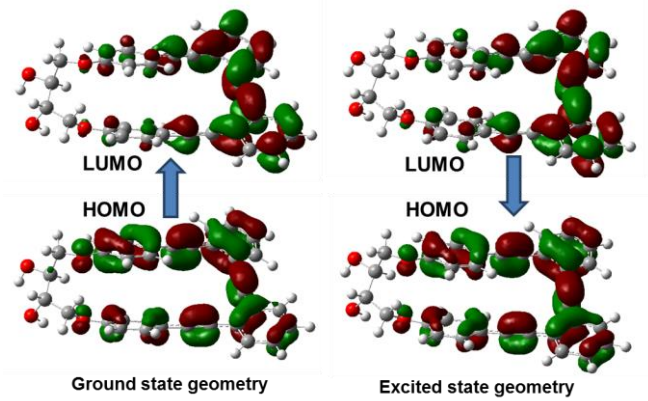

Figure 9. Isovalue orbital surfaces for HOMO (bottom) and LUMO (top) orbitals in the ground state geometry (left) and excited state geometry (right) of compound (*P,S,S*)-**1**.

VCD

To gain further information and to test the theoretical conformational study, we considered also the use of VCD spectra.[33-45] VCD is very sensitive to conformations of compounds in solution and to conformational mobility, due to the fact that vibrational chiroptical response can reflect also local differences and may heavily depend on hindered torsions.[33-35] Therefore, VCD gives relevant structural information about the sample in solution, which in many cases cannot be inferred from

other spectroscopic techniques. Moreover, infrared, in contrast to UV spectroscopy, is quite sensitive to the conformation of the aliphatic part of the molecule: the bridge and the substituents. In this case we selected for the study representative compounds (*P*,*P*,*S*)-**2** (Figure 10) and (*P*,*P*,*S*)-**3** (Figure 11).

The most intense VCD features are assigned to normal modes delocalized between the methyl of the acetyl groups and in-plane bendings of the nearby phenyls (negative features at 1230-1247 cm^{-1} for compound (*P*,*P*,*S*)-**2**; 1233 cm^{-1} for compound (*P*,*P*,*S*)-**3**, positive feature at 1237 cm^{-1} for compound (*P*,*P*,*S*)-**3**) and to vibrations involving methynes of the asymmetric carbons and adjacent methylenes (positive feature at 1269 cm^{-1} for compound (*P*,*P*,*S*)-**2**, with OH bending contribution, and 1283 cm^{-1} for compound (*P*,*P*,*S*)-**3**).

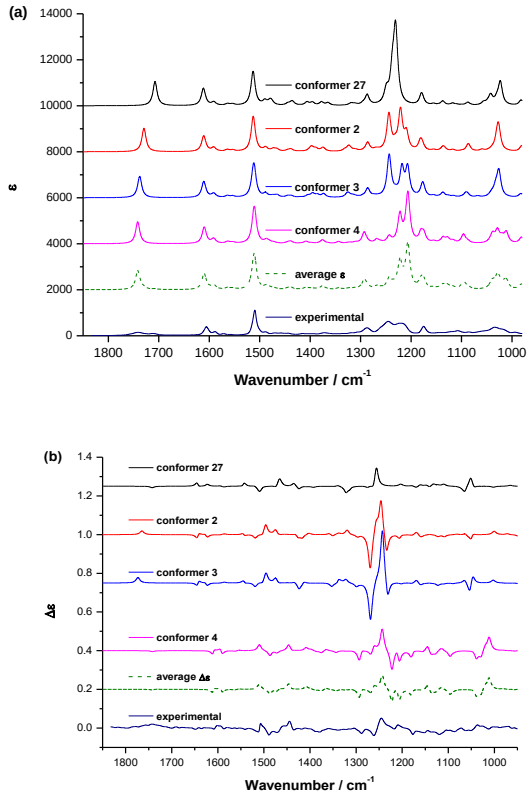

FIGURE 10. (a) Infrared and (b) VCD spectra for compound (*P*,*P*,*S*)-**2**: experimental data, calculated average (considering energy Boltzmann populations) on the four main conformers (iefpcm B3LYP/TZVP), calculated spectra of the four most populated conformers (see SI). Calculated spectra wavelengths have been scale by 0.98, Lorentzian band shape has been assumed with 10 cm^{-1} half-width.

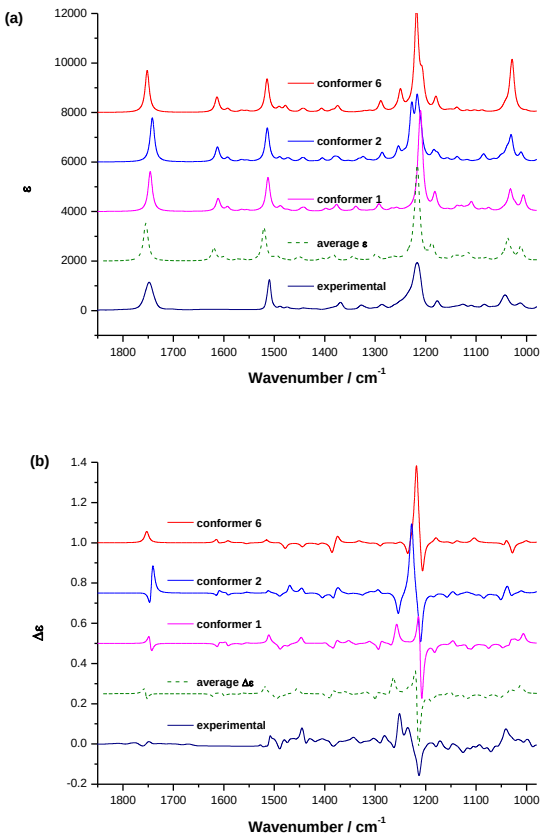

FIGURE 11. (a) Infrared and (b) VCD spectra for compound (*P*,*P*,*S*)-**3**: experimental data, calculated average (considering energy Boltzmann populations) on the four main conformers (iefpcm B3LYP/TZVP), calculated spectra of the four most populated conformers (see SI). Calculated spectra wavelengths have been scale by 0.98, Lorentzian band shape has been assumed with 10 cm^{-1} half-width

Experimental data (navy blue lines) are quite well matched by DFT calculations (olive green dashed lines). In both cases, averages obtained with Boltzmann factors on calculated energy give a better fit than the ones obtained by Gibbs free energy.

As can be seen, similar VCD spectra are obtained for compounds (*P*,*P*,*S*)-**2** and (*P*,*P*,*S*)-**3**, (apart from the more intense negative feature at 1230 cm^{-1} for (*P*,*P*,*S*)-**3**). In both compounds helix conformation and staple conformation are almost identical and the structural differences are due to the presence of one or two acetyl groups and their spatial layout. The OPE helical scaffold favors just one conformation of the staple-bridge in para position irrespective of the substituents, as documented by tables in SI. It is also noticeable that, considering the two symmetric compounds (*P*,*P*,*S*)-**3** and (*P*,*P*,*S*)-**5,** the two CO groups are symmetrically arranged on opposite sides and lay in the same plane. The structure calculated for compound (*P*,*P*,*S*)-**5** in solution is nearly superimposable to the structure found in the crystal. All these findings support the idea of that helical scaffold is the main responsible of the optical properties of this family of compounds.

Conclusion

In this paper we have demonstrated that a simple and straightforward structure based on an enantiopure *o*-oligo(PhenyleneEthynylene) (o-OPE) diol derivative (*P*,*S*,*S*)-**1** is a robust and strong CPL emitter with g_{lum} values up to 1.1 x10^{-2}. The introduction of bulky substituents in one or both hydroxyl groups does not affect to the chiroptical properties of the derivatives neither in the ground nor in the excited state. Moreover, DFT and TD-DFT calculations are in good agreement with experimental results, showing that ECD and CPL spectra of this family of compounds are strictly related with the OPE backbone, with negligible influence of the steric hindrance or local conformations of different substituents. Due to this fact, this structure could be further functionalized to obtain compounds with groups able to carry out sensing processes (pH, detection or quantitation probes) without losing CPL emission. Research on this topic is currently on-going in our group.

Materials and Methods

Synthesis. General Details. Drying of organic extracts was performed over anhydrous Na_2SO_4. TLC was performed on aluminium-backed plates coated with silica gel 60 (230-240 mesh) with F254 indicator. The spots were visualized with UV light (254 nm). All chromatography purifications were performed with silica gel 60 (40-60 μm). NMR spectra were measured at room temperature. ^{1}H NMR spectra were recorded at 400, 500 or 600 MHz. Chemical shifts are reported in ppm using residual solvent peak as reference ($CHCl_3$: δ = 7.26 ppm, CH_2Cl_2: δ = 5.32 ppm). Data are reported as follows: chemical shift, multiplicity (s: singlet, d: doublet, t: triplet, q: quartet, quint: quintuplet, m: multiplet, dd: doublet of doublets, dt: doublet of triplets, dq: doublet of quartets, td: triplet of doublets, bs: broad singlet), coupling constant (*J* in Hz) and integration; ^{13}C NMR spectra were recorded at 100, 125 or 150 MHz using broadband proton decoupling, and chemical shifts are reported in ppm using residual solvent peaks as reference ($CHCl_3$: δ = 77.16 ppm, CH_2Cl_2: δ = 54.0 ppm). Carbon multiplicities were assigned by DEPT techniques. High resolution mass spectra (HRMS) were recorded on a mass spectrometer using EI at 70eV. The known compound (*P*,*S*,*S*)-**1** was isolated as pure sample and showed NMR spectra matching those of previously reported.[30]

Compound (*P*,*S*,*S*)-2. To a solution of the diol (*P*,*S*,*S*)-**1**(50 mg, 0.101 mmol) in CH_2Cl_2 (2 mL), dimethylaminopyridine (DMAP) (25 mg, 0.202 mmol) and Ac_2O (9 mg, 0.081 mmol) were added. The mixture was stirred for 24 h at room temperature. Then, CH_2Cl_2 was added, and the mixture was washed with water, dried, and the solvent was removed. The residue was purified by flash chromatography (EtOAc/Hexane 2:8) to give monoacetate (*P*,*S*,*S*)-**2** (49 mg, 56%). White solid: ^{1}H NMR (400 MHz, $CDCl_3$, δ): 7.66-7.61 (m, 2H), 7.61-7.56 (m, 2H), 7.34-7.29 (m, 4H), 7.29-7.10 (m, 4H), 6.53 (d, *J* = 8.7 Hz, 2H), 6.42 (d, *J* = 8.7 Hz, 2H), 5.28-5.34 (m, 1H), 4.39-4.32 (m, 2H), 4.25-4.20 (m, 1H), 4.15-4.00 (m, 2H), 2.20 (s, 3H); ^{13}C NMR (100 MHz, $CDCl_3$, δ):170.5 (C), 157.0 (C), 156.8 (C), 133.6 (CH), 133.53 (CH), 133.48 (CH), 132.8 (CH), 132.7 (CH), 130.2 (CH), 128.3 (CH), 128.2 (CH), 127.7 (CH), 127.6 (CH), 125.4 (C), 125.3 (C), 125.1 (C), 125.0 (C), 116.0 (C), 115.9 (C), 114.5 (CH), 114.3 (CH), 93.9 (C), 93.8 (C), 92.5 (C), 92.4 (C), 87.5 (C), 69.3 (CH), 66.5 (CH), 62.96 (CH_2), 62.95 (CH_2), 21.1 (CH_3)·; HRMS (ESI, m/z): $[M + Na]^+$ calcd. for $C_{36}H_{26}O_5Na$, 561.1672; found, 561.1686.

Compound (*P*,*S*,*S*)-3. To a solution of the diol (*P*,*S*,*S*)-**1** (40 mg, 0.088 mmol) in CH_2Cl_2 (10 mL), DMAP (43 mg, 0.35 mmol) and Ac_2O (27 mg, 0.26 mmol) were added. The mixture was stirred for 24 h at room temperature. Then, the solvent was removed. The residue was purified by flash chromatography (EtOAc/Hexane 2:8) to give diacetate (*P*,*S*,*S*)-**3** (51 mg, 83%). White solid: ^{1}H NMR (600 MHz, $CDCl_3$, δ): 7.64-7.61 (m, 2H), 7.60-7.58 (m, 2H), 7.34-7.28 (m, 8H), 6.55 (d, *J* = 8.7 Hz, 4H), 5.46-5.40 (m, 2H), 4.37 (dd, *J* = 11.6, 3.2 Hz, 2H), 4.01 (dd, *J* = 11.6, 8.4 Hz, 2H), 2.18 (s, 6H); ^{13}C NMR (150 MHz, $CDCl_3$, δ): 170.4 (C), 156.7 (C), 133.6 (CH), 133.5 (CH), 132.8 (CH), 128.2 (CH), 127.6 (CH), 125.4 (C), 125.1 (C), 116.2 (C), 114.5 (CH), 93.9 (C), 92.4 (C), 87.5 (C), 67.3 (CH), 63.2 (CH_2), 21.0 (CH_3); HRMS (ESI, m/z): $[M + Na]^+$ calcd. for $C_{38}H_{28}O_6Na$, 603.1778; found, 603.1777.

Compound (*P*,*S*,*S*)-4. To a solution of the diol (*P*,*S*,*S*)-**1** (50 mg, 0.101 mmol) in CH_2Cl_2 (2 mL), DMAP (25 mg, 0.202 mmol) and pivaloyl chloride (PivCl) (11 mg, 0.091 mmol) were added. The mixture was stirred for 24 h at room temperature. Then, CH_2Cl_2 was added, and the mixture was washed with water, dried, and the solvent was removed. The residue was purified by flash chromatography (EtOAc/Hexane 2:8) to give monopivaloyl (*P*,*S*,*S*)-**4** (53 mg, 57%). White solid: ^{1}H NMR (400 MHz, $CDCl_3$, δ): 7.68-7.54 (m, 3H), 7.34-7.27 (m, 9H), 6.56 (d, *J* = 8.6 Hz, 2H), 6.42 (d, *J* = 8.6 Hz, 2H), 5.30 (dt, *J* = 9.1, 4.0 Hz, 1H), 4.37 (dd, *J* = 11.3, 3.7 Hz, 1H), 4.32 (dd, *J* = 11.3, 3.7 Hz, 1H), 4.23 (dt, *J* = 9.1, 4.0 Hz, 1H), 4.14-3.97 (m, 2H), 1.7-1.5 (brs, OH), 1.31 (s, 9H); ^{13}C NMR (100 MHz, $CDCl_3$, δ): 178.1 (C), 157.1 (C), 156.8 (C), 133.6 (CH), 133.5 (CH), 133.4 (CH), 132.8 (CH), 132.7 (CH), 128.3 (CH), 128.2 (CH), 127.7 (CH), 127.6 (CH), 125.4 (C), 125.3 (C), 125.1 (C), 125.0 (C), 116.0 (C), 115.9 (C), 114.5 (CH), 114.3 (CH), 93.9 (C), 93.8 (C), 92.5 (C), 92.4 (C), 87.5 (C), 68.6 (CH), 66.8 (CH), 66.5 (CH_2), 62.9 (CH_2), 39.3 (C), 27.4 (CH_3); HRMS (ESI, m/z): $[M + Na]^+$ calcd. for $C_{39}H_{32}O_5Na$, 603.2141; found, 603.2128.

Compound (*P*,*S*,*S*)-5. To a solution of the diol (*P*,*S*,*S*)-**1** (30 mg, 0.06 mmol) in CH_2Cl_2 (6 mL), DMAP (44 mg, 0.36 mmol) and PivCl (30 mg, 0.24 mmol) were added. The mixture was stirred for 24 h at room temperature. Then, the solvent was removed. The residue was purified by flash chromatography (EtOAc/Hexane 2:8) to give dipivaloyl (*P*,*S*,*S*)-**5** (34 mg, 85%). Yellow oil: ^{1}H RMN (400 MHz, CD_2Cl_2, δ): 7.67-7.65 (m, 1H), 7.65 (d, *J*= 2.4 Hz, 1H), 7.63 (d, *J* = 2.4 Hz, 1H), 7.62-7.60 (m, 1H), 7.39-7.32 (m, 4H), 7.31-7.26 (m, 4H), 6.60-6.55 (m, 4H), 5.43-5.36 (m, 2H), 4.33-4.29 (m, 2H), 4.00-3.89 (m, 2H), 1.28 (s, 18H). ^{13}C RMN (100 MHz, CD_2Cl_2, δ): 178.2 (C), 157.3 (C), 134.0 (CH), 133.9 (CH), 133.2 (CH), 128.8 (CH), 128.2(CH), 125.8 (C), 125.3 (C), 116.3 (C), 115.1 (CH), 94.3 (C), 92.7 (C), 87.7 (C), 67.1 (CH), 63.3 (CH_2), 39.5 (C), 27.5 (CH_3); HRMS (ESI, m/z): $[M + H]^+$ calcd. for $C_{44}H_{40}O_6Na$, 687.2717; found, 687.2703.

Compound (*P*,*S*,*S*)-6. To a solution of the diol (*P*,*S*,*S*)-**1** (40 mg, 0.081 mmol) in CH_2Cl_2 (2 mL), imidazol (8 mg, 0.122 mmol) and *tert*-buthyl dimethyl silyl chloride (TBSCl) (29 mg, 0.097 mmol) were added. The mixture was stirred for 24 h at room temperature. Then, CH_2Cl_2 was added, and the mixture was washed with water, dried, and the solvent was removed. The residue was purified by flash chromatography (EtOAc/Hexane 2:8) to give monosilylated

derivative (*P*,*S*,*S*)-**6** (39 mg, 82%). Colourless oil: ^{1}H NMR(500 MHz, $CDCl_3$, δ): 7.65-7.56 (m, 4H), 7.35-7.28 (m, 8H), 6.48 (d, *J* = 8.4 Hz, 2H), 6.41 (d, *J* = 8.4 Hz, 2H), 4.32 (dd, *J* = 11.9, 4.4 Hz, 1H), 4.20-4.01 (m, 4H), 3.81 (t, *J* = 11.9 Hz, 1H), 0.97 (s, 9H), 0.26 (s, 3H), 0.23 (s, 3H); ^{13}C NMR (125 MHz, $CDCl_3$, δ): 156.7 (C), 133.62 (CH), 133.60 (CH), 133.54 (CH), 133.50 (CH), 132.7 (CH), 132.6 (CH), 128.3 (CH), 128.2 (CH), 127.6 (CH), 125.5 (C), 125.4 (C), 125.1 (C), 125.0 (C), 115.8 (C), 115.7 (C), 114.5 (CH), 114.4 (CH), 93.9 (C), 93.8 (C), 92.4 (C), 92.3 (C), 87.6 (C), 87.5 (C), 65.5 (CH), 65.0 (CH_2), 64.9 (CH_2), 64.8 (CH), 25.9 (CH_3), 18.2 (C), -4.0 (CH_3), -4.6 (CH_3); HRMS (ESI, m/z): $[M + Na]^+$ calcd. for $C_{40}H_{38}O_4SiNa$, 633.2431; found, 633.2437.

UV, ECD, CPL, IR and VCD measurements. Identical solutions (about 0.7 10^{-4} M in CH_2Cl_2) were used first for ECD and then for CPL measurements using a microfluorescence quartz cuvette 2x10 mm. A Jasco 815SE apparatus was employed for ECD measurements (time constant = 2 sec, monochromator velocity 100 nm/min,1 scan). For CPL measurements we employed the homemade instrument described in previous papers[3,4]; the excitation radiation (340nm) was brought to the cell from a Jasco FP8200 fluorimeter through an optical fibre containing water. A 90° scattering geometry was adopted.

IR and VCD spectra were taken with a Jasco FVS6000 FTIR spectrometer equipped with a VCD module, comprised of a wire-grid linear polarizer, a ZnSe Photo Elastic Modulator (PEM) to produce 50 kHz modulated circularly polarized radiation and a liquid N_2-cooled MCT detector. The spectra were taken for 0.04-0.05 M CD_2Cl_2 solutions, in 200 μm BaF2 cells. 5000 scans were taken for each spectra and subtraction of VA and VCD spectra of the solvent were performed.

Fluorescence quantum yields and lifetime measurements. Quinine in 0.1M H_2SO_4 was used as reference (Φ_r = 0.54) and fluorescence quantum yields were calculated by registering absorbance and integrated fluorescence spectra of compounds (*P*,*S*,*S*)-**1**-**6** and quinine in different solvents (See SI for more details). Time-resolved fluorescence decay traces were collected using a 375 nm laser pulse as excitation source and for the necessary time to reach 20,000 counts at the peak channel. They were recorded in single photon timing (SPT) mode on a FluoTime 200 fluorometer. The fluorescence decay traces were fitted to a two- or three-exponential function, by using a Levenberg-Marquard algorithm-based nonlinear least-squares error minimization deconvolution method.

Theoretical calculations. Accurate molecular mechanics (MM) conformational search was performed for all OPE molecules, assuming (1*S*, 2*S*) configuration. All structures within 8 kcal/mol were optimized at B3LYP/6-31G* level. Populated conformers were optimized also within the framework of polarizable continuum model approximation (PCM), checking that all structures correspond to minima and evaluating the Gibbs free energy. The time-dependent DFT (TD-DFT) method has been used to calculate Absorption and CD spectra at the same level of approximation, iefpcm B3LYP/6-31G*. All calculations were performed with Gaussian09 package.[46]

Acknowledgements

We thank MICINN (CTQ2014-53598-R) and Junta de Andalucía (FQM1484) for financial support. Computing Center CINECA Via Magnanelli 6/3 40033 – Casalecchio di Reno (Bologna) Italy and Regione Lombardia for the LISA Grant No. "ChiPhyto: HPL13POZE1" is acknowledged for access to computational facilities. P. Reiné thanks MICINN for a FPU fellowship.

This paper is dedicated to Ettore Castiglioni who significantly contributed to the development of the CPL technique and actively participated to the collaboration of the two groups in Granada and Brescia.

Supporting information

Additional supporting information may be found in the online version of this article at the publisher's website.

REFERENCES AND NOTES

1. Riehl JP, Muller G. Circularly polarized luminescence spectroscopy and emission-detected circular dichroism. In: Berova N, Polavarapu PL, Nakanishi K, Woody RW. *Comprehensive Chiroptical Spectroscopy*. John Wiley & Sons;**2012**, vol. 1:p. 65-90.

2. Sanchez-Carnerero EM, Agarrabeitia AR, Moreno F,Maroto BL, Muller G, Ortiz MJ, de la Moya S. Circularly polarized luminescence from simple organic molecules. *Chem Eur J* **2015**;*21*:13488-13500.

3. Castiglioni E, Abbate S, Longhi G. Revisiting with updated hardware an old spectroscopic technique: circularly polarized luminescence. *Appl Spectrosc* **2010**;*64*:1416-1419.

4. Castiglioni E, Abbate S, Lebon F, Longhi G. Chiroptical spectroscopic techniques based on fluorescence. *Methods Appl Fluoresc* **2014**; 2:024006.

5. Kumar J, Nakashima T, Kawai T. Circularly polarized luminescence in chiral molecules and supramolecular assemblies. *J Phys Chem Lett* **2015**; 6:3445-3452.

6. Longhi G, Castiglioni E, Koshoubu J, Mazzeo G, Abbate S. Circularly polarized luminescence: A review of experimental and theoretical aspects. *Chirality* **2016**;*28*:696-707.

7. Peeters E, Christiaans PT, Janssen RAJ, Schoo HFM, Dekkers HPJM, Meijer EW. Circularly polarized electroluminescence from a polymer light-emitting diode. *J Am Chem Soc* **1997**;*119*:9909-9910.

8. Satrijo A, Meskers SCJ, Swager TM. Probing a Conjugated Polymer's Transfer of Organization-Dependent Properties from Solutions to Films. *J Am Chem Soc* **2006**;*128*:9030-9031.

9. Liu J, Su H, Meng L, Zhao Y, Deng C, Ng JCY, Lu P, Faisal M, Lam JWY, Huang X, Wu H, Wong KS, Tang BZ. What makes efficient circularly polarised luminescence in the condensed phase: aggregation-induced circular dichroism and light emission. *Chem Sci* **2012**;*3*:2737-2747.

10. San Jose BA, Yan J, Akagi K. Dynamic switching of the circularly polarized luminescence of disubstitutedpolyacetylene by selective transmission through a thermotropic chiral nematic liquid crystal. *Angew Chem Int Ed* **2014**;*53*:10641-10644.

11. Frawley AT, Pal R, Parker D. Very bright, enantiopure europium(III) complexes allow time-gated chiral contrast imaging. *Chem Commun* **2016**;*52*:13349-13352

12. Zinna F, Giovanella U, Di Bari L. Highly circularly polarized electroluminescence from a chiral europium complex. *Adv Mater* **2015**;*27*:1791-1795.

13. Brandt JR, Wang X, Yang Y, Campbell AJ, Fuchter MJ. Circularly polarized phosphorescent electroluminescence with a high dissymmetry factor from PHOLEDs based on a platinahelicene. *J Am Chem Soc* **2016**;*138*:9743-9746.

14. Schulte TR, Holstein JJ, Krause L, Michel R, Stalke D, Sakuda E, Umakoshi K, Longhi G, Abbate S, Clever G. Chiral-at-Metal Phosphorescent

Square-Planar Pt(II)-Complexes from an Achiral Organometallic Ligand. *J Am Chem Soc* **2017**;*139*:6863-6866.

15. Hellou N, Srebro-Hooper M, Favereau L, Zinna F, Caytan E, Toupet L, Dorcet V, Jean M, Vanthuyne N, Williams JAG, Di Bari L, Autschbach J, Crassous J. Enantiopure Cycloiridiated Complexes Bearing a Pentahelicenic N-Heterocyclic Carbene and Displaying Long-Lived Circularly Polarized Phosphorescence. *Angew Chem Int Ed* **2017**;*56*: 8236-8239.

16. Shen C, Srebro-Hooper M, Jean M, Vanthuyne N, Toupet L, Wiliams JAG, Torres AR, Riives AJ, Muller G, Autschbach J, Crassous J. Synthesis and chiroptical properties of hexa-, octa-, and deca-azaborahelicenes: Influence of helicene size and of the number of boron atoms. *Chem Eur J* **2017**;*23*:407-418.

17. Sawada Y, Furumi S, Takai A, Takeuchi M, Noguchi K, Tanaka K. Rhodium-catalyzed enantioselective synthesis, crystal structures, and photophysicalproperties of helically chiral 1,1′-bitriphenylenes. *J Am Chem Soc* **2012**;*134*:4080-4083.

18. Sánchez-Carnerero EM, Moreno F, Marto BL, Agarrabeitia AR, Ortiz MJ, Vo BG, Muller G, de la Moya S. Circularly polarized luminescence by visible-light absorption in a chiral O-BODIPY dye: Unprecedented design of CPL organic molecules from achiral chromophores. *J Am Chem Soc* **2014**;*136*:3346-3349.

19. Morisaki Y, Gon M, Sasamori T, Tokitoh N, Chujo Y. Planar chiral tetrasubstituted [2.2]paracyclophane: Optical resolution and functionalization. *J Am Chem Soc* **2014**;*136*:3350-3353.

20. Shen C, Anger E, Srebo M, Vanthuyne N, Deol KK, Jefferson Jr TD, Muller G, Williams JAG, Toupet L, Roussel C, Autschbach J, Reau R, Crassous J. Straightforward access to mono- and bis-cycloplatinated helicenes displaying circularly polarized phosphorescence by using crystallization resolution methods. *Chem Sci* **2014**;*5*:1915-1927.

21. Inouye M, Hayashi K, Yonenaga Y, Itu T, Fujimoto K, Uchida T, Iwamura M, Nozaki K. A doubly alkynylpyrene-threaded [4]rotaxane that exhibits strong circularly polarized luminescence from the spatially restricted excimer. *Angew Chem Int Ed* **2014**;*53*:14392-14396.

22. Nakamura K, Furumi S, Takeuchi M, Shibuya T, Tanaka K. Enantioselective synthesis and enhanced circularly polarized luminescence of S-shaped double azahelicenes. *J Am Chem Soc* **2014**;*136*:5555-5558.

23. Kögel JF, Kusada S, Sakamoto R, Iwashima T, Tsuchiya M, Toyoda R, Matsuoka R, Tsukamoto T, Yuasa J, Kitagawa Y, Kawai T, Nishihara H. Heteroleptic [bis(oxazoline)](dipyrrinato)zinc(II) complexes: bright and circularly polarized luminescence from an originally achiral dipyrrinato ligand. *Angew Chem Int Ed* **2016**;*55:*1377-1381.

24. Hirata S, Vacha M. Circularly polarized persistent room-temperature phosphorescence from metal-free chiral aromatics in air. *J Phys Chem Lett* **2016**;*7*:1539-1545.

25. Hernandez-Delgado I, Pascal S, Wallabregue A, Duwald R, Besnard C, Guénée L, Nançoz C, Vauthey E, Tovar RC, Lunkley JL, Muller G, Lacour J. Functionalized cationic [4]helicenes with unique tuning of absorption, fluorescence and chiroptical properties up to the far-red range. *Chem Sci* **2016**;*7:*4685-4693

26. Feuillastre S, Pauton M, Gao L, Desmarchelier A, Riives AJ, Prim D, Tondelier D, Geffroy B, Muller G, Clavier G, Pieters G. Design and synthesis of new circularly polarized thermally activated delayed fluorescence emitters. *J Am Chem Soc* **2016**;*138*:3990-3993.

27. Xiong JB, Feng HT, Sun JP, Xie WZ, Yang D, Liu M, Zheng YS. The fixed propeller-like conformation of tetraphenylethylene that reveals aggregation-induced emission effect, chiral recognition, and enhanced chiroptical property. *J Am Chem Soc* **2016**;*138*:11469-11472.

28. Toyoda M, Imai Y, Mori T. Propeller Chirality of Boron Heptaaryldipyrromethene: Unprecedented supramolecular dimerization and chiroptical properties. *J Phys Chem Lett* **2017**;*8*:42-48.

29. Jiménez J, Cerdán L, Moreno F, Maroto BL, García-Moreno I, Lunkley JL, Muller G, de la Moya S. Chiral organic dyes endowed with circularly polarized laser emission. *J Phys Chem C* **2017**;*121*:5287-5292.

30. Morcillo SP, Miguel D, Álvarez de Cienfuegos L, Justicia J, Abbate S, Castiglioni E, Bour C, Ribagorda M, Cárdenas DJ, Paredes JM, Crovetto L, Choquesillo-Lazarte D, Mota AJ, Carreño MC, Longhi G, Cuerva JM. Stapled helical o-OPE foldamers as new circularly polarized luminescence emitters based on carbophilic interactions with Ag(I)-sensitivity. *Chem Sci* **2016**;*7*:5663-5670.

31. Fuentes N, Martín-Lasanta A, Álvarez de Cienfuegos L, Robles R, Choquesillo-Lazarte D, García-Ruiz JM, Martínez-Fernández L, Corral I, Ribagorda M, Mota AJ, Cárdenas DJ, Carreño MC, Cuerva JM. Versatile bottom-up approach to stapled π-conjugated helical scaffolds: Synthesis and chiroptical properties of cyclic o-phenyleneethynylene oligomers. *Angew Chem Int Ed* **2012**;*51*:13036-13040.

32. Furche F, Ahlrichs R, Wachsmann C, Weber E, Sobanski A, Vögtle F,Grimme G. Circular Dichroism of Helicenes Investigated by Time-Dependent Density Functional Theory. *J Am Chem Soc* **2000**;*122*:1717-1724.

33. Setnicka V, Urbanova M, Bouř P, Kral V, Volka K. Vibrational Circular Dichroism of 1,1‘-Binaphthyl Derivatives: Experimental and Theoretical Study. *J Phys Chem A* **2001**;*105*:8931−8938.

34. Abbate S, Burgi LF, Castiglioni E, Lebon F, Longhi G, Toscano F, Caccamese S. Assessment of configurational and conformational properties of naringenin by vibrational circular dichroism. *Chirality* **2009**;*21*:436−441.

35. Passarello M, Abbate S, Longhi G, Lepri S, Ruzziconi R,Nicu VP. Importance of C*–H Based Modes and Large Amplitude Motion Effects in Vibrational Circular Dichroism Spectra: The Case of the Chiral Adduct of Dimethyl Fumarate and Anthracene. *J Phys Chem A* **2014**;*118*:4339−4350

36. Nafie LA, *Vibrational Optical Activity, Principles and applications*. John Wiley&Sons Ltd. **2011**, NY. Polavarapu PL, *Chiroptical Spectroscopy, Fundamentals and Applications*. CRC Press, Taylor and Francis Group, **2017**, BocaRaton, FL.

37. Stephens PJ, Devlin FJ, Cheeseman JR. *VCD Spectroscopy for Organic Chemists*. CRC Press: BocaRaton, FL. **2012**

38. Yang GC, Xu Y. Vibrational Circular Dichroism Spectroscopy of Chiral Molecules. *Top Curr Chem* **2011**;*298*:189-236.

39. Polavarapu PL. Structural Analysis Using Chiroptical Spectroscopy: Insights and Cautions. *Chirality* **2016**;*28*:445-452.

40. Taniguchi T, Hongen T, .Monde K. Studying the stereostructures of biomolecules and their analogs by vibrational circular dichroism. *Polym J* **2016**;48:925–931.

41. Taniguchi T, Nakano K, Baba R, Monde K. Analysis of Configuration and Conformation of Furanose Ring in Carbohydrate and Nucleoside by Vibrational Circular Dichroism. *Org Lett* **2017**;*19*:404-407.

42. Bultinck PFL, Cherblanc MJ, Fuchter MJ, Herrebout WA, Lo YP, Rzepa HS, Siligardi G, Weimar M. Chiroptical Studies on Brevianamide B: Vibrational and Electronic Circular Dichroism Confronted. *J Org Chem* **2015**;*80*:3359-3367.

43. Buffeteau TL, Ducasse L., Poniman L, Delsuc N, Huc I. Vibrational circular dichroism and ab initio structure elucidation of an aromatic foldamer. *Chem Commun* **2006**;2714-2716.

44. Losada M, Xu Y. Chirality transfer through hydrogen-bonding: Experimental and ab initio analyses of vibrational circular dichroism spectra of methyl lactate in water. *Phys Chem Chem Phys* **2007**;*9*:3127-3135.

45. Longhi G, Abbate S, Gangemi R, Giorgio E, Rosini C. Fenchone, Camphor, 2-Methylenefenchone and 2-Methylenecamphor: A Vibrational Circular Dichroism Study. *J Phys Chem A* **2007**; *110*:4958-4968.

46. Frisch MJ, Trucks GW, Schlegel HB, Scuseria GE, Robb MA, Cheeseman JR., Scalmani G, Barone V, Mennucci B, Petersson GA, Nakatsuji H, Caricato M, Li X, Hratchian HP, Izmaylov AF, Bloino J, Zheng G, Sonnenberg JL, Hada M, Ehara M, Toyota K, Fukuda R, Hasegawa J, Ishida M, Nakajima T, Honda Y, Kitao O, Nakai H, Vreven T, Montgomery JA, Peralta Jr JE, Ogliaro F, Bearpark M, Heyd JJ, Brothers E, Kudin KN, Staroverov VN, Kobayashi R, Normand J, Raghavachari K, Rendell A, Burant JC, Iyengar SS, Tomasi J, Cossi M, Rega N, Millam JM, Klene M, Knox JE, Cross JB, Bakken V, Adamo C, Jaramillo J, Gomperts R, Stratmann RE, Yazyev O, Austin AJ, Cammi R, Pomelli C, Ochterski JW, Martin RL, Morokuma K, Zakrzewski VG, Voth GA, Salvador P, Dannenberg JJ, Dapprich S, Daniels AD, Farkas Ö, Foresman JB, Ortiz JV, Cioslowski J, Fox DJ. Gaussian 09 Revision D.01, Gaussian Inc. Wallingford CT, **2009**.

Graphical Abstract

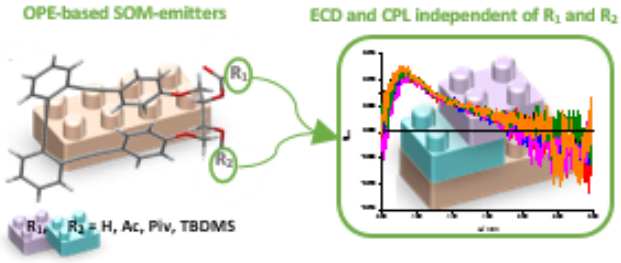

((A graphical abstract is used in each issue's online graphical table of contents must be included in all manuscripts. The image may be a key figure or a scheme from the text; it may be a reaction, equation, concept, etc. or an imaginative illustration of a concept described in the manuscript, preferably in color. Spectra or other analytical data are not recommended. The image will be printed square with sides not larger than 2 inches/5 cm; the use of graphs and images consisting of several parts is therefore strongly discouraged.))